

Cite this: *Polym. Chem.*, 2021, **12**, 5139

# Polyesters with bio-based ferulic acid units: crosslinking paves the way to property consolidation†

Doris Pospiech,<sup>a</sup> Andreas Korwitz,<sup>a</sup> Hartmut Komber,<sup>a</sup> Dieter Jehnichen,<sup>a</sup> Kerstin Arnhold,<sup>a</sup> Harald Brüning,<sup>a</sup> Holger Scheibner,<sup>a</sup> Michael T. Müller<sup>a</sup> and Brigitte Voit<sup>a,b</sup>

Aromatic–aliphatic polyesters can be prepared as bio-based materials by incorporating monomers from biogenic sources. Here, 2-methyl (*E*)-3-(4-(2-hydroxyethoxy)-3-methoxyphenyl)acrylate, a derivative of ferulic acid, was synthesised and inserted into the structure of aliphatic and aromatic–aliphatic polyesters as a comonomer. Terpolymers with high relative molar masses  $M_w$  from 50 000 to 100 000 g mol<sup>-1</sup> can be successfully prepared by transesterification polycondensation in the melt. Incorporation of ferulate units with intact double bonds is proven by NMR spectroscopy. Insertion of low molar amounts of ferulate units reduces the crystallinity of the base polyesters, but enhances the glass transition temperature. It is demonstrated that the materials after melt processing to a suitable shape (fibres, parts, films) can be crosslinked by electron beam irradiation, which enhances the stability of the materials.

Received 24th June 2021,  
Accepted 16th August 2021

DOI: 10.1039/d1py00851j

rsc.li/polymers

## 1 Introduction

Over the years, the development and utilization of bio-based polymers have gained significant attention in an effort to increase the sustainability of the plastics industry.<sup>1</sup> Bio-based polymers originate exclusively from natural biomass as the only source of renewable carbon.<sup>2</sup> The main feedstocks are natural polymers that occur directly in nature (for instance cellulose and chitosan), plant oils, natural rubber, food feedstock (so-called sugar platform) and biomass that remains after industrial extraction of cellulose.<sup>2,3</sup> Lignocellulose is the most abundant natural polymer.<sup>4</sup> After extracting the cellulose, a lignin-rich liqueur remains to about 14–30 wt% forming the second most abundant source of natural polymers and the most important source for renewable aromatic compounds, among them furans, terpenes, and monolignols (*p*-coumaryl alcohol, sinapyl alcohol and coniferyl alcohol).<sup>3,5–8</sup> So far, the only industrial process to generate pure low molar mass compounds out of lignin is the production of vanillin (4-hydroxy-3-methoxybenzaldehyde) from liginosulfonate *via* sulphite

pulping<sup>7</sup> or, more recently, by electrochemical transformation of Kraft lignin<sup>9</sup> to vanillin. Vanillin can easily be converted into several monomers, thus forming a significant chemical platform for synthesis of bio-based polymers.<sup>1,7,10–13</sup> Two of the most important derivatives are 4-hydroxy-3-methoxybenzoic acid and 2-methyl-hydroquinone which have frequently been used as comonomers for polyesters.<sup>11,12,14–18</sup> Mialon *et al.*,<sup>12</sup> for instance, converted vanillin into poly(dihydroferulic acid), a bio-based analogue of poly(ethylene terephthalate).

Another interesting monomer that is either incorporated directly into the lignin structure (for instance in plants such as *Pinus radiata* and *Populus tremula x Populus Alb*), or is converted from coniferaldehyde (from lignin) *via* oxidation by hydroxyl-cinnamaldehyde dehydrogenase, is the bifunctional monomer ferulic acid (FA, (*E*)-3-(4-hydroxy-3-methoxy-phenyl) acrylic acid or 4-hydroxy-3-methoxy-cinnamic acid), an hydroxycarboxylic acid.<sup>19</sup> FA acid has been reported to show antimicrobial,<sup>20</sup> antioxidant<sup>21</sup> and even anticancer<sup>22</sup> properties that are ascribed to the phenolic structure of the compound.

A few attempts exist in which ferulic acid was subjected directly to polycondensation. Llevot *et al.*<sup>7</sup> reported homopolyesters based on FA. The weight-averaged molar masses  $M_w$  were in most cases below 10 000 g mol<sup>-1</sup>. Ouimet *et al.*<sup>23,24</sup> protected the carboxylic group by a *tert*-butyl group and reacted the OH group with carboxylic acid dichlorides. Deprotection of

<sup>a</sup>Leibniz-Institut für Polymerforschung Dresden e.V., Hohe Str. 6, 01069 Dresden, Germany. E-mail: pospiech@ipfdd.de

<sup>b</sup>Organic Chemistry of Polymers, Technische Universität Dresden, 01069 Dresden, Germany

†Electronic supplementary information (ESI) available. See DOI: 10.1039/d1py00851j





The degradation behaviour was investigated by thermogravimetric analysis (TGA) with a Q 5000 (TA Instruments, USA) in the temperature range 30 to 800 °C with a heating rate of 10 K min<sup>-1</sup> under nitrogen.

Wide-angle X-ray scattering (WAXS) profiles were recorded in symmetric transmission using the 2-cycle diffractometer XRD 3003 T/T (GE Sensing & Inspection Technologies GmbH, Ahrensburg, Germany). The measurements were conducted at 40 kV and 30 mA, CuK $\alpha$  radiation (monochromatised with Goebel mirror,  $\lambda = 0.15418$  nm) with the following parameters:  $2\theta$ -range: 0.5–45°; measuring time per measuring point: 30 s; step size  $\Delta 2\theta$ : 0.05°, room temperature. Samples were wrapped in Al foil or filled in glass tubes ( $\varnothing = 1$  mm). For calculation of the crystallinity  $\alpha$ , based on the intensity parts scattered by crystalline as well as amorphous amounts peak-fitting with pseudo-Voigt functions was executed by using the software package Analyze (included in RayfleX, software of the X-ray device).

Raman measurements were performed on melt-pressed samples using RAMAN Imaging System WITec alpha300R (WITec GmbH, Ulm, Germany) equipped with 785 nm laser (10 mW). 200 accumulations with integration time of 0.5 s were recorded for one spectrum.

The shore hardness of melt-pressed samples (thickness 4 mm, diameter 25 mm) was analysed by means of a Zwick 3140 device (Zwick GmbH & Co. KG, Ulm, Germany) according to DIN EN ISO 868 Shore D (15 s). The tensile strength of fibres was measured by an UPM Zwick-2.5 kN instrument (Zwick GmbH & Co. KG, Ulm, Germany) with a measuring velocity of 1 mm min<sup>-1</sup> until deformation.

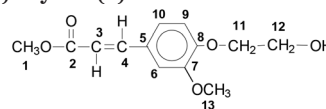
### Synthesis of methyl (*E*)-3-(4-hydroxy-3-methoxyphenyl)acrylate

The synthesis was performed according to the procedure described by Kreye *et al.*<sup>30</sup> Ferulic acid (10 g, 51.5 mmol) was dissolved in methanol (50 mL, 1.236 mol) in a one-neck flask equipped with condenser and magnetic stirrer. Concentrated sulphuric acid (0.5 mL, 9.38 mmol) was added under vigorous stirring and the reaction mixture was refluxed for four hours. After that time, the solution was cooled, neutralised with sodium hydrogen carbonate and filtered. The reaction solution was added to ethyl acetate and shaken several times in a separating funnel with saturated sodium hydrogen carbonate solution. Finally, it was treated with saturated sodium chloride solution and the organic phase was dried with sodium sulphate. Ethyl acetate was removed from the dried organic phase and the product was dried under reduced pressure at 50 °C overnight.

Yield: 90%. The product was obtained as dark brown, highly viscous liquid, which crystallises upon standing at room temperature.

<sup>1</sup>H NMR (DMSO-*d*<sub>6</sub>):  $\delta = 9.55$  (br s, 1H; OH), 7.56 (d, 15.9 Hz, 1H; =CH-Ph), 7.31 (d, 2.0 Hz, 1H; H<sub>Ar</sub>), 7.12 (dd, 8.3 Hz, 2.0 Hz, 1H; H<sub>Ar</sub>), 6.79 (d, 8.3 Hz, 1H; H<sub>Ar</sub>), 6.45 (d, 15.9 Hz, 1H; =CH-C(O)), 3.82 (s, 3H; PhOCH<sub>3</sub>), 3.70 ppm (s, 3H; C(O)OCH<sub>3</sub>).

### Synthesis of methyl (*E*)-3-(4-(2-hydroxyethoxy)-3-methoxyphenyl)acrylate (F)



Ethylene carbonate (15.851 g, 180 mmol), methyl (*E*)-3-(4-hydroxy-3-methoxyphenyl)acrylate (24.985 g, 120 mmol), dimethylacetamide (125.5 mL, 1.349 mol) and potassium iodide (0.478 g, 2.88 mmol) were placed in a two-necked flask with condenser and magnetic stirrer. The mixture was heated to 150 °C under nitrogen flow and under vigorous stirring. The reaction proceeded at this temperature for three hours. After completion, the mixture was cooled down and a large excess of iced water was added under vigorous stirring. The precipitate was filtered off after one day of stirring, washed with water and dried at 50 °C under reduced pressure.

Yield: 85%. The product was obtained as beige solid. Mp.: 99 °C.

<sup>1</sup>H NMR (DMSO-*d*<sub>6</sub>):  $\delta = 7.59$  (d, 15.9 Hz, 1H; 4), 7.34 (d, 2.0 Hz, 1H; 6), 7.22 (dd, 8.4 Hz, 2.0 Hz, 1H; 10), 6.99 (d, 8.4 Hz, 1H; 9), 6.55 (d, 15.9 Hz, 1H; 3), 4.84 (t, 5.5 Hz, 1H; OH), 4.02 (t, 4.9 Hz, 2H; 11), 3.81 (s, 3H; 13), 3.72 (m, 2H; 12), 3.71 ppm (s, 3H; 1) (ESI Fig. 1†).

<sup>13</sup>C NMR (DMSO-*d*<sub>6</sub>):  $\delta = 167.0$  (2), 150.5 (8), 149.2 (7), 144.8 (4), 126.9 (5), 122.9 (9), 115.3 (3), 112.7 (10), 110.8 (6), 70.3 (11), 59.6 (12), 55.6 (13), 51.3 ppm (1) (ESI Fig. 2†).

### Terpolyester synthesis

The melt polycondensations were carried out on laboratory scale in a three-necked 100 mL-glass flask equipped with mechanical stirrer, nitrogen inlet and distillation bridge. The monomers (dried overnight at 50 °C under reduced pressure) and catalysts (see Table 1, catalyst amount: 1 wt% based on the total weight of the monomers) were added to the flask in the appropriate composition (molar ratio dimethyl ester/diol/ferulic acid methyl ester according to Table 1). The flask was evacuated and flushed three times with nitrogen and was then placed in a metal bath pre-heated to 150 °C. Transesterification was carried out under stirring in nitrogen atmosphere with a continuous temperature raise within 60 min to 245 °C (series P(T-Pr-F), P(T-iPr-F), P(T-B-F) and P(S-B-F)) or 270 °C (series P(T-E-F)), respectively. The melt was stirred for 30 min under moderate nitrogen flow after the final reaction temperature was reached. Polycondensation was carried out with stirring under reduced pressure (10 Pa–5 Pa) for 30 min or, respectively, the time given in Table 1. At the end of the reaction, the flask was filled with nitrogen, taken out of the metal bath and the product was removed mechanically. Average yield: 90%.

Selected samples were upscaled by polycondensation in a 2.4 L stirring autoclave (Juchheim Laborgeräte GmbH, Bernkastel Kues, Germany). The dried monomers and catalysts were given in the appropriate proportions into the agitated autoclave pre-heated to 150 °C. The autoclave was closed, evacuated and flushed with nitrogen three times, and then the



**Table 1** Synthesis conditions, molecular characteristics, X-ray crystallinity  $\alpha$  and thermal behaviour of copolyesters containing ferulate units

Polymer	Molar ratio <sup>b</sup> T-diol-F (mol%/mol%/mol%)	Cat. <sup>c</sup>	$t^d$ (h)	$M_n^e$ (g mol <sup>-1</sup> )	$M_w^e$ (g mol <sup>-1</sup> )	$M_w/M_n$	$\eta_{inh}^f$ (dL g <sup>-1</sup> )	$\alpha^g$	$T_g^h$ (°C)	$T_m^h$ (°C)	$\Delta H_m^h$ (J g <sup>-1</sup> K <sup>-1</sup> )
P(T-E) [PET] <sup>a</sup>	50.8/49.2/0	1	7	37 000	83 000	2.24	0.72	0.69	84	222/253	53.4
P(T-E-F)-2	47.4/48.3/4.3	1	3	28 000	68 000	2.43	0.63	0	78	225/236	34.5
P(T-E-F)-4	45.6/46.1/8.3	1	3	15 000	67 000	4.47	0.60	0	79	169 211	-12.0 13.3
P(T-E-F)-6	32.7/32.7/34.6	1	3	13 000	142 000	10.92	<sup>i</sup>	0.42	81	—	—
P(T-Pr) [PTT] <sup>a</sup>	39.5/60.5/0	2	7	62 000	138 000	2.24	1.27	0.64	57	220/228	66.0
P(T-Pr-F)-2	47.7/47.7/4.6	2	1	25 000	73 000	2.92	0.90	0	60	217	44.8
P(T-Pr-F)-4	45.7/45.4/8.9	2	1	22 000	95 000	4.32	0.95	<sup>j</sup>	72	173	34.3
P(T-Pr-F)-7	32.8/33.8/33.4	2	1	21 000	108 000	5.14	0.84	0	74	—	—
P(T-iPr)	50.0/50.0/0	2	3	8 000	21 000	2.62	0.26	0	80	—	—
P(T-iPr-F)-1	48.2/47.3/4.5	2	1	19 000	87 000	4.58	0.76	0	81	—	—
P(T-iPr-F)-2	45.5/45.5/9.0	2	1	21 000	95 000	4.52	0.78	0	90	209	0.8
P(T-iPr-F)-6	33.0/33.7/33.3	2	0.5	18 000	107 000	5.94	<sup>i</sup>	0	92	—	—
P(T-B) [PBT] <sup>a</sup>	50.3/49.7/0	3	7	32 000	78 000	2.44	0.90	0.54	42	—	—
P(T-B-F)-1	48.0/47.7/4.3	3	3	15 000	53 000	3.53	0.69	0.28	49	—	—
P(T-B-F)-2	46.6/45.7/7.7	3	3	19 000	79 000	5.27	0.95	0	53	—	—
P(T-B-F)-4	33.3/34.0/32.7	3	1	24 000	91 000	3.79	<sup>i</sup>	<sup>j</sup>	66	—	—
<b>S-diol/F</b>											
P(S-B) [PBS] <sup>a</sup>	50.0/50.0/0	2	3	41 000	93 000	2.27	0.90	0.37	-35	111/114	71.8
P(S-B-F)-2	45.5/48.2/6.3	1	3	10 000	22 000	2.20	0.36	—	-27	37/76 97	-41.2 46.1
P(S-B-F)-5	42.9/45.8/11.3	1	3	12 400	19 600	2.11	0.41	0	-15	—	—
P(S-B-F)-7	30.5/34.4/35.1	1	1	11 000	53 000	4.82	0.37	0	29	—	—
P(F) <sup>k</sup>	0/0/100	3	3	1700	2800	1.65	0.10	0.71	80	223	40.3

<sup>a</sup> Conventional name of the homopolyesters. <sup>b</sup> Determined by <sup>1</sup>H NMR spectroscopy; estimated error  $\pm$  0.5 mol%. <sup>c</sup> Catalyst, 1: potassium acetate; 2: mixture of titanium tetrabutylate and antimony trioxide (1:1 wt/wt); 3: titanium tetrabutylate, (1 wt% with respect to the total monomer weight). <sup>d</sup> Polycondensation time under reduced pressure. <sup>e</sup> Determined by SEC. <sup>f</sup> Determined by viscometry. <sup>g</sup> Determined by WAXS. <sup>h</sup> Determined by DSC, 2<sup>nd</sup> heating. All experimental details are given in the Experimental section. <sup>i</sup> Not completely soluble. <sup>j</sup> Not measured. <sup>k</sup> Synthesised at 150 °C.

transesterification was started under stirring and moderate nitrogen flow. The autoclave was heated to 200 °C within 10 min, the temperature was maintained at 200 °C for 20 min before heating up to 245 °C (series P(T-Pr-F), P(T-iPr-F), P(T-B-F) and P(S-B-F)) or 280 °C (series P(T-E-F)), respectively, within 45 min or 60 min, respectively. The polycondensation reaction was continued under moderate nitrogen flow for four hours or seven hours, respectively. After that time, the autoclave was allowed to cool down. Then, the material was mechanically removed and ground.

### Melt spinning

Melt spinning was performed with a self-constructed piston-type spinning device equipped with a 0.2 mm nozzle (capillary diameter) as described earlier.<sup>31</sup> The polymer was dried before processing at 80 °C for 4 h under reduced pressure. The spinning temperature was set to 240 °C, the take-up speed (winding speed) was 100 m min<sup>-1</sup>, and the resulting fibres had a diameter of about 80  $\mu$ m.

### Preparation of samples for electron beam treatment and mechanical tests

Before processing, the materials were dried at 50 °C for 12 hours under reduced pressure. The samples for e-beam treatment and mechanical tests (hardness) were melt pressed using a Specac press (Specac Ltd Science and Innovation Centre, Orpington, UK) with hydraulic Atlas foil pressing tool

between two polyimide sheets separated by a spacer ring (100  $\mu$ m) at 200 °C with a weight of 4000 kg for one minute. The films were cooled to room temperature in a water-cooled case. The final thicknesses of the transparent films were in the range of 50–70  $\mu$ m and had a diameter of 2 cm.

### Electron beam (EB) treatment of terpolyester films

The samples were irradiated in a special irradiation chamber<sup>32</sup> using an electron accelerator ELV-2 (Budker Institute of Nuclear Physics, Novosibirsk, Russia<sup>33</sup>). Before irradiation, the samples were dried at 50 °C for 8 hours under reduced pressure in a vacuum oven. After the drying process, the copolyester samples were placed into the irradiation chamber. Before irradiation, the chamber was heated up to 80 °C and kept for 5 minutes under reduced pressure to remove moisture and oxygen. Subsequently, the chamber was cooled down or heated up to the target irradiation temperatures (25 °C, 110 °C or 160 °C, respectively) in nitrogen atmosphere. The irradiation was carried out with constant electron energy (1.5 MeV) and electron current (4 mA), the dose was applied by several steps of 25 kGy until the target dose was reached. After the electron beam treatment, the samples were cooled down under nitrogen and subsequently taken out of the irradiation chamber.

### Determination of the gel content

The irradiated samples (120 mg) were dissolved in a mixture of PFP/CHCl<sub>3</sub> (1:1 v/v, 15 mL) and stirred for 4 h. The solvent



was removed and a new portion (15 mL) was added. The samples were again stirred for 48 h. Then, the gel content was separated by filtration, washed with chloroform and dried at 50 °C under reduced pressure for 60 h, and the mass was determined.

### 3 Results and discussion

#### Terpolyester synthesis and characterisation

FA was first converted into the methyl ester followed by reaction with ethylene carbonate to obtain methyl (*E*)-3-(4-(2-hydroxyethoxy)-3-methoxyphenyl)acrylate (denominated as F), see Fig. 1, eqn (1). The polycondensation of this activated monomer with dimethyl terephthalate or dimethyl succinate, respectively, and aliphatic diols was examined (Fig. 1, eqn (2)) and yielded five series of copolyesters (1: P(T-E-F) with ethylene glycol as the diol; 2: P(T-Pr-F) with 1,3-propanediol as the diol; 3: P(T-iPr-F) with 1,2-propanediol as the diol; 4: P(T-B-F) with 1,4-butanediol as the diol; and 5: P(S-B-F)) with dimethyl succinate and 1,4-butanediol as comonomers. The polycondensation was performed in melt (melt transesterification polycondensation) under the conditions briefly mentioned in Table 1.

Both, the final temperature and the time for polycondensation at this temperature depended on the structure of the comonomers. Series P(T-E-F) required 270 °C (in accordance to PET<sup>34</sup>), the other series were prepared by a final polycondensation temperature of 245 °C, as for PBT<sup>35</sup> and PBS.<sup>36</sup> The standard polycondensation time under reduced pressure was three hours (seven hours in the up-scaled experiments in a 2.4 L stirring autoclave). For the copolyesters with the highest content of F the polycondensation times had to be shorter to suppress crosslinking (1 h for P(T-Pr-F)-7, 0.5 h for P(T-iPr-F)-6, and 1 h for P(T-B-F)-4.

First, the homopolymerisation of methyl (*E*)-3-(4-(2-hydroxyethoxy)-3-methoxyphenyl)acrylate (F) was attempted. The NMR spectra (ESI Fig. 3–5†) proved condensation occurred for

sample P(F), but intense methylester and hydroxyethyl signals revealed that only oligomers were formed.

In contrast, the copolymerisation of F with diacids (T, S) and diols (E, Pr, iPr and B) resulted in terpolymers with a composition in very good agreement with the composition expected from monomer feed ratio. The molar ratios of the three monomers of the terpolymers (Table 1) were determined from appropriate <sup>1</sup>H NMR signals as given in the ESI (section 2.2†). Apparently, the incorporation of the F comonomer into the polyesters occurred without problems, at least up to contents of about 35 mol%. All polymers were characterised by <sup>1</sup>H NMR spectroscopy and spectra and signal assignments are compiled in the ESI (Fig. 6, 9, 12, 15 and 18†). <sup>13</sup>C NMR spectra were recorded only from one polymer of each series for more detailed structure confirmation (ESI Fig. 7, 10, 13, 16 and 19†). The <sup>13</sup>C NMR signal assignments are based on the evaluation of 1D and of 2D NMR spectra (ESI Fig. 8, 11, 14, 17 and 20†). For example, Fig. 2 depicts the <sup>1</sup>H spectrum and two regions of the <sup>13</sup>C NMR spectrum of P(T-Pr-F)-7. The <sup>1</sup>H NMR spectrum agrees with the expected structure, and side reactions of the acrylic moiety of F could not be detected, which is also true for the other polymers. In contrast to the copolymers from diacid and diol with alternating monomer units in the backbone, the incorporation of F with an acid and alcohol functionality results in a more complex microstructure (ESI, section 1†). As indicated in Fig. 2, several <sup>1</sup>H and <sup>13</sup>C NMR signals show splitting due to the different dyads or triads. For all terpolymers with highest F content, a quantitative evaluation of several diad and triad contents, respectively, revealed



**Fig. 1** Synthesis of ferulic acid methyl (*E*)-3-(4-(2-hydroxyethoxy)-3-methoxyphenyl)acrylate (eqn (1)) used as monomer for the copolycondensation with dimethyl terephthalate or dimethyl succinate, respectively, and aliphatic diols (eqn (2)).



**Fig. 2** (a) <sup>1</sup>H NMR spectrum and (b) two regions of the <sup>13</sup>C NMR spectrum of P(T-Pr-F)-7 (33.4 mol% F; solvent: CDCl<sub>3</sub>:TFA-d 4:1 v/v). Assignments to diad and triad signals are given.



that a random distribution of the monomers occurred and no formation of longer F sequences could be stated.

The molar masses and dispersity of the copolyesters were measured by size exclusion chromatography (SEC). The solvent mixture used (pentafluorophenol/chloroform) only allowed the calculation of molar masses relative to polystyrene standards and not the use of a light scattering detector. The elution curves of all polyesters (ESI Fig. 21–25†) were unimodal.

The relative molar masses in the P(T-E-F) series and in the P(T-B-F) series were not significantly affected by the ferulate comonomer at molar F concentrations up to 8 mol%, yielding  $M_w$  values up to 95 000 g mol<sup>-1</sup>. In contrast, the relative molar masses in the P(S-B-F) series were significantly lower than for the starting PBS. The samples of all series with the highest amount of ferulate units in the range of 30 mol% showed a higher dispersity  $M_w/M_n$  and higher  $M_w$ . It is assumed that this might be caused by side reactions of the double bond. The double bonds may have polymerised thermally to a very low extent and thus caused long-chain branching which alters the dispersity of the sample.

The general trend of the SEC results is also reflected by the solution viscosities ( $\eta_{inh}$ ) that were measured in the same solvent mixture of pentafluorophenol/chloroform.

It can be summarised at this point that the polycondensations undertaken yielded copolyester samples with intact double bonds and molar masses in the typical range of standard polyesters.

### Solid state structure

The solid state structure of the as-synthesised terpolyesters was analysed by WAXS to outline the influence of ferulate units. The main focus of the work was on samples with low molar content of F. The influence of the F content is discussed for the P(T-E-F) series as an example. The WAXS curves are displayed in Fig. 3. The curve for the homopolymer PET (curve 1) corresponds to those reported in the literature.<sup>34,37–39</sup> The oligomeric ferulate homopolymer P(F) (curve 5) also exhibited a

semicrystalline structure. A comparison from literature could not be found. The variety of reflections might be caused by the low molar mass of the sample presumably containing contributions of monomer crystallinity. However, this sample represents a necessary control for the terpolyesters P(T-E-F). The incorporation of low molar amounts of ferulate units into the PET structure (4.3 mol% in P(T-E-F)-2, curve 2; and 8.3 mol% in P(T-E-F)-4, curve 3) resulted in a drastic reduction of crystallinity  $\alpha$  to zero (see Table 1). An enhanced molar content of 34.6 mol% in P(T-E-F)-6, curve 4, yielded a polymer with a new type of crystalline structure that is neither the one of PET, nor the one of P(F) (curve 5). This special crystalline structure has not been observed in the other terpolyester series.

The WAXS curves of all other polymer series are displayed in the ESI (ESI Fig. 26–28†). Incorporation of F in the P(T-Pr-F) series resulted in complete disappearance of crystallinity (ESI Fig. 26†). In contrast, the series P(T-iPr-F) was completely amorphous due to the amorphous nature of the homopolymer P(T-iPr) caused by the suppression of crystallinity by the methyl substituent (ESI Fig. 27†). Incorporation of low molar amounts of F into PBT (5.3 mol% in P(T-E-F)-1) preserved the PBT crystallinity, but at a somewhat lower degree (ESI Fig. 28†).

### Melting behavior

DSC was employed to support the results of the X-ray measurements and to analyse the melting behaviour of the terpolyesters. The second heating run was used to exclude the influences of the thermal history of the samples. The parameters determined ( $T_g$ ,  $T_m$ ,  $\Delta H_m$ ) are summarised in Table 1.

Fig. 4 shows as example the DSC curves of the P(T-E-F) series.

The DSC curve of the PET control (P(E-T)) reflects the thermal behaviour known from literature<sup>34,40</sup> with a glass transition temperature  $T_g$  at 84 °C and a main melting peak  $T_m$  at 253 °C. Incorporation of ferulate units reduced both, the



Fig. 3 WAXS patterns of the copolyester series P(T-E-F), 1: P(T-E) (PET); 2: P(T-E-F)-2 (4.3 mol% F); 3: P(T-E-F)-4 (8.3 mol% F); 4: P(T-E-F)-6 (34.6 mol% F); 5: P(F). Curves shifted for better visualisation.



Fig. 4 DSC curves (2<sup>nd</sup> heating) of the terpolyesters P(T-E-F) with different molar content of F.



melting peak maximum  $T_m$  as well as the melting enthalpy  $\Delta H_m$ . This crystallinity was not present in the as-synthesised samples, in accordance with the WAXS results, but was generated in the recrystallisation during the first heating. The sample P(T-E-F)-6 only showed a glass transition within the measuring range until 300 °C. It is assumed that the melting of this special crystalline structure containing F units occurs far above 300 °C, similar to poly(hydroxybenzoic acid).<sup>41,42</sup> A comparable behaviour was observed for the P(T-Pr-F) series (ESI Fig. 29†).

The series P(T-iPr-F) showed only glass transitions, in accordance with the WAXS findings. ESI Fig. 30† illustrates that both, glass transition temperature as well as  $\Delta c_p$  increased with increasing F content. This behaviour was observed in all series. PBT showed two melting peaks as described earlier.<sup>36</sup> Incorporation of 4.3 mol% F shifted the maxima to lower temperature, but preserved the basic behaviour (ESI Fig. 31†). This is again following the WAXS results that proved the preserved PBT crystallinity in the sample. Higher amounts of F suppressed the crystallinity. The melting peak maxima  $T_m$  of the series show the following tendency: P(T-E-F) > P(T-Pr-F) > P(T-B-F) > P(S-B-F). The DSC curves of P(S-B-F) are displayed in ESI Fig. 32.† The incorporation of ferulate units enhanced in all series the glass transition temperature (except for PET, where the homopolymer PET had the highest  $T_g$ ) as shown in Fig. 5. The  $T_g$  of the low molar mass homopolymer P(F) was found to be 80 °C, lower than reported by Nguyen *et al.*<sup>43</sup> However, it should not be overestimated because of the low molar mass of the sample.

### Thermal stability of the terpolyesters

The thermal stability of the polyesters is of high importance for most of the applications and was further examined by TGA. The complete data are summarized in ESI Table 1.† The thermogravimetric curves of series P(T-Pr-F) are displayed in



Fig. 5 Influence of the molar content of ferulate units F on the  $T_g$  of the terpolyester series.



Fig. 6 TGA curves of the terpolyesters of series P(T-Pr-F).

Fig. 6, the curves of the other series are given in the ESI (Fig. 33–36†).

The thermal decomposition maximum shifted to higher temperature with increasing F comonomer content. This is explained by the enhancement of stability caused by the incorporation of aromatic F units. The influence of the spacer on the decomposition maxima was clearly visible and raised in the following order: P(T-iPr-F) < P(T-Pr-F) and P(T-B-F) < P(T-E-F), in accordance to the tendency found for the homopolyesters.<sup>36</sup> Additionally, the residue obtained after measurement at 800 °C (char) enhanced with increasing F content, see Fig. 7. The only exception was found in the P(T-E-F) series where the char of the homopolymer P(T-E) was the highest which is due to the very special decomposition mechanism of PET resulting in a significant amount of aromatic ring structures.<sup>44</sup>

In summary, the TGA results indicated a higher thermostability of terpolyesters compared to homopolyesters by incorporation of ferulate units. This is taken as a first indication to a more favourable fire behaviour. All copolyesters are stable until 300 °C.

### Study of crosslinkability by electron beam treatment

The ability to polymerise the double bond in the F units of the terpolyesters after polycondensation and melt processing was studied using the P(T-E-F) series and one sample of the P(T-B-F) series as representative samples. The monomeric FA is a sterically hindered 1,2-disubstituted acrylic monomer. Thus, it is not expected to easily undergo thermal polymerisation. Only a few reports described thermal copolymerisation with styrene initiated by the radical initiator azobis(isobutyronitrile) (AIBN), resulting in rather low molar mass oligomers.<sup>45</sup>

Preliminary experiments with the sample P(T-E-F)-2 in solution and bulk at 250 °C did not yield any sign of crosslinking. The same was observed after UV irradiation. Thus, we choose for the study presented the method of e-beam irradiation (EB). Initial experiments with sample P(T-E-F)-2 at room tempera-





Fig. 7 Influence of the molar content of F units on the residue after TGA at 800 °C.

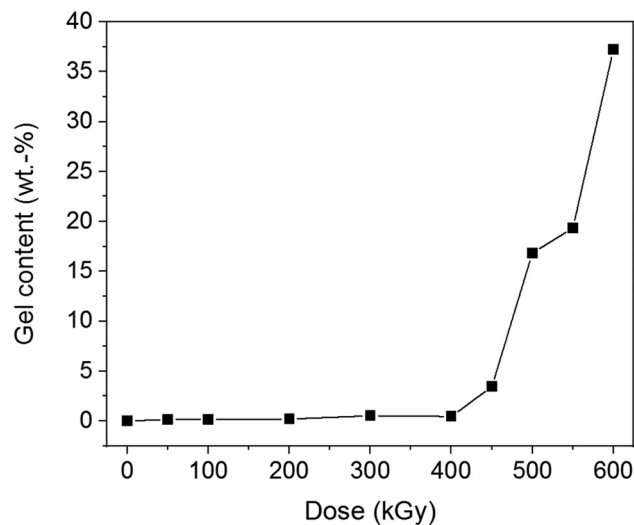


Fig. 8 Influence of the applied EB dose on the gel content in sample P(T-E-F)-2.

ture with doses between 100 and 600 kGy also did not result in crosslinking. Consequently, the melt-pressed copolyester samples as well as the melt-pressed non-modified homopolymers (PET and PBT) were irradiated at a temperature above  $T_g$  (typically 110–120 °C) to ensure high molecular mobility of the polymer chains in the amorphous phase. Different doses up to 600 kGy were applied and the resulting samples were evaluated using solubility in the solvent mixture PFP/CHCl<sub>3</sub> after 45 min. The photographic images of all irradiated samples are shown in ESI Fig. 37,† their appearance in PFP/CHCl<sub>3</sub> (gel contents) are summarised in ESI Fig. 38.†

All non-irradiated samples independent of their F content were completely soluble in PFP/CHCl<sub>3</sub>. Increasing F content yielded melt-pressed films with a brownish colour (ESI Fig. 37†). PET and PBT films were transparent and remained colourless after EB treatment with all doses. They were completely soluble in PFP/CHCl<sub>3</sub> after EB irradiation. That means, EB treatment did not cause significant changes in the chemical structure of PET and PBT and no crosslinking. Irradiated samples of the P(T-E-F) series showed partial crosslinking, visible by swollen, gelled parts in PFP/CHCl<sub>3</sub>. The gel content was enhanced with both increasing F content as well as increasing dose (ESI Fig. 38†), which is demonstrated in Fig. 8 for sample P(T-E-F)-2 with 4.3 mol% F.

Samples P(T-B-F)-1 showed comparable behaviour (ESI Fig. 39†). Selected samples were analysed before and after EB irradiation by Raman spectroscopy. The double bond in the starting sample P(T-E-F)-2 was only weakly visible by broadening of the band at 1645 cm<sup>-1</sup>. EB irradiation resulted in a very weak change of this shoulder (ESI Fig. 40†), which cannot be taken as proof of the reaction of the double bonds.

The results discussed above demonstrated that melt-processed terpolyesters with F comonomers can be successfully crosslinked by EB treatment.

Table 2 Tensile test results of as-spun and EB treated fibres of the sample P(T-E-F) with 4.3 mol% F units

Polymer P(T-E-F)-2	$E_t$ (MPa)	$\sigma_m$ (MPa)	$\epsilon_b$ (%)
As-spun	4200 ± 137	28.7 ± 9.7	0.6 ± 0.2
EB treated (600 kGy)	4286 ± 69	57.6 ± 7.6	1.4 ± 0.2

### Mechanical tests

Selected copolyesters were melt-pressed to obtain samples for a preliminary evaluation of mechanical properties and the influence of EB treatment. Hardness tests (Shore D and compression tests) did not reveal significant differences between the samples. The shore D hardness of the F-containing sample P(T-E-F)-2 was comparable to PET (see ESI Table 2†). No influence of EB treatment was observed. This could be due to the thickness of the sample which exceeded the irradiation depth by several times. Therefore, melt-spun fibres of sample P(T-E-F)-2 were further analysed with and without EB treatment, to determine whether fibres as thinner samples would show a more pronounced effect of EB treatment. The fibre thickness of about 80 μm allowed complete irradiation of the sample volume. The values of the tensile tests of non-treated and EB treated fibres are summarised in Table 2, the stress-strain curves are given in ESI Fig. 40 and 41.†

The preliminary experiments showed an increase of  $E_t$ , tensile strength  $\sigma_m$  and elongation at break  $\epsilon_b$  after EB treatment. The stress-strain curves are given in ESI Fig. 41 and 42.† Detailed examinations will be performed in the future.

## 4 Conclusions

In this contribution, terpolyesters based on PET, PBT, PTT, PiPrT, PBS and containing ferulate units were reported. The



terpolyesters could be prepared successfully by transesterification copolycondensation without thermal polymerisation of the double bonds and yielded soluble products. This is, to the best of our knowledge, the first report about such polyesters with significant molar content of ferulate units. The chemical structure of the terpolyesters were studied in detail by NMR spectroscopy and SEC. These methods demonstrated that high molar mass polyesters with unimodal molar mass distribution and random monomer sequences were formed.

The incorporation of ferulate units had significant influence on the reduction of crystallinity, which can only be preserved in the PBT series at low molar contents of about 5 mol%. In contrast, the glass transition temperatures raised with increasing content of ferulate, indicating a better thermostability of the terpolyesters. Crosslinking by EB treatment occurred *via* the double bonds of the terpolyester, proven by the fact that the base homopolyesters could not be crosslinked by EB irradiation.

In summary, it can be stated that incorporation of bio-based ferulate units into conventional copolyesters enhances the sustainability of polyester materials and adds interesting aspects into the property profile, in particular, the opportunity to crosslink materials after thermoplastic processing, successfully demonstrated here by EB treatment. EB treatment resulted in crosslinking within the surface layers of the materials and is most effective in fibres, but also offers the opportunity to stabilise injection-moulded or 3D printed parts.

## Author contributions

Conceptualization: D. P., A. K. and D. J.; Data curation: D. P., A. K., H. K. and D. J.; Funding acquisition: D. P.; Investigation: D. P., A. K., H. K., D. J., K. A., H. B., H. S. and M. T. M.; Methodology: D. P. and D. J.; Project administration: D. P.; Resources: D. P. and B. V.; Supervision: D. P. and B. V.; Validation: D. P., H. K. and D. J.; Visualization: D. P., D. J. and K. A.; Writing – original draft: D. P., A. K.; H. K., D. J., M. T. M. and B. V.; Writing – review & editing: D. P. and D. J.

## Conflicts of interest

There are no conflicts to declare.

## Acknowledgements

Financial support by Deutsche Forschungsgemeinschaft (project number PO 575/13-1) is gratefully acknowledged. Furthermore, the authors wish to thank Mrs Petra Treppe (IPF) for SEC measurements, Mrs Julia Muche (IPF) for Raman measurements, and Norbert Smolka (IPF) for fibre spinning of sample P(T-E-F)-2.

## Notes and references

- H. Nakajima, P. Dijkstra and K. Loos, *Polymers*, 2017, **9**, 1–26.
- E. Piorowska, *Adv. Polym. Sci.*, 2019, 1–35.
- R. M. O’dea, J. A. Willie and T. H. Epps, *ACS Macro Lett.*, 2020, **9**, 476–493.
- G. W. Huber, S. Iborra and A. Corma, *Chem. Rev.*, 2006, **106**, 4044–4098.
- L. Costes, F. Laoutid, S. Brohez and P. Dubois, *Mater. Sci. Eng., R*, 2017, **117**, 1–25.
- S. Laurichesse and L. Avérous, *Prog. Polym. Sci.*, 2014, **39**, 1266–1290.
- A. Llevot, E. Grau, S. Carlotti, S. Grelier and H. Cramail, *Macromol. Rapid Commun.*, 2016, **37**, 9–28.
- P. Azadi, O. R. Inderwildi, R. Farnood and D. A. King, *Renewable Sustainable Energy Rev.*, 2013, **21**, 506–523.
- F. S. Chakar and A. J. Ragauskas, *Ind. Crops Prod.*, 2004, **20**, 131–141.
- M. Fache, E. Darroman, V. Besse, R. Auvergne, S. Caillol and B. Boutevin, *Green Chem.*, 2014, **16**, 1987–1998.
- M. Firdaus and M. A. R. Meier, *Eur. Polym. J.*, 2013, **49**, 156–166.
- L. Mialon, R. Vanderhenst, A. G. Pemba and S. A. Miller, *Macromol. Rapid Commun.*, 2011, **32**, 1386–1392.
- A. G. Pemba, M. Rostagno, T. A. Lee and S. A. Miller, *Polym. Chem.*, 2014, **5**, 3214–3221.
- L. H. Bock and J. K. Anderson, *J. Polym. Sci.*, 1958, **28**, 121–127.
- W. Lange and O. Kordsachia, *Holz Roh- Werkst.*, 1981, **39**, 107–112.
- H. R. Kricheldorf and G. Löhden, *Polymer*, 1995, **36**, 1697–1705.
- F. Pion, P. H. Ducrot and F. Allais, *Macromol. Chem. Phys.*, 2014, **215**, 431–439.
- C. H. R. M. Wilsens, J. M. G. A. Verhoeven, B. A. J. Noordover, M. R. Hansen, D. Auhl and S. Rastogi, *Macromolecules*, 2014, 3306–3316.
- R. Rinaldi, R. Jastrzebski, M. T. Clough, J. Ralph, M. Kennema, P. C. A. Bruijninx and B. M. Weckhuysen, *Angew. Chem., Int. Ed.*, 2016, **55**, 8164–8215.
- R. Puupponen-Pimiä, L. Nohynek and C. Meier, *J. Appl. Microbiol.*, 2001, **90**, 494–507.
- H. R. El-Seedi, A. M. A. El-Said, S. A. M. Khalifa, U. Göransson, L. Bohlin, A. K. Borg-Karlson and R. Verpoorte, *J. Agric. Food Chem.*, 2012, **60**, 10877–10895.
- S. Ou and K. C. Kwok, *J. Sci. Food Agric.*, 2004, **84**, 1261–1269.
- M. A. Ouimet, J. J. Faig, W. Yu and K. E. Uhrich, *Biomacromolecules*, 2015, **16**, 2911–2919.
- M. A. Ouimet, J. Griffin, A. L. Carbone-Howell, W. H. Wu, N. D. Stebbins, R. Di and K. E. Uhrich, *Biomacromolecules*, 2013, **14**, 854–861.
- B. M. Upton and A. M. Kasko, *Chem. Rev.*, 2016, **116**, 2275–2306.



- 26 M. Schwarzer, A. Korwitz, H. Komber, L. Häußler, B. Dittrich, B. Schartel and D. Pospiech, *Macromol. Mater. Eng.*, 2018, **303**, 1–16.
- 27 O. Fischer, D. Pospiech, A. Korwitz, K. Sahre, L. Häußler, P. Friedel, D. Fischer, C. Harnisch, Y. Bykov, M. Döring, L. Häußler, P. Friedel, D. Fischer, C. Harnisch, Y. Bykov and M. Döring, *Polym. Degrad. Stab.*, 2011, **96**, 2198–2208.
- 28 S. C. Ligon, R. Liska, J. Stampfl, M. Gurr and R. Mülhaupt, *Chem. Rev.*, 2017, **117**, 10212–10290.
- 29 M. Vaezi, H. Seitz and S. Yang, *Int. J. Adv. Des. Manuf. Technol.*, 2013, **67**, 1721–1754.
- 30 O. Kreye, S. Oelmann and M. A. R. Meier, *Macromol. Chem. Phys.*, 2013, **214**, 1452–1464.
- 31 D. Pospiech, A. Korwitz, K. Eckstein, H. Komber, D. Jehnichen, M. Suckow, A. Lederer, K. Arnhold, M. Göbel, M. Bremer, A. Hoffmann, S. Fischer, A. Werner, T. Walther, H. Brüning and B. Voit, *J. Appl. Polym. Sci.*, 2019, **136**, 48257.
- 32 H. Körber, U. Lappan, U. Geißler, K. Lunkwitz and R. Hanke, Institute of Polymer Research Dresden, DE19930742A1, 1999.
- 33 H. Dorschner, W. Jenschke and K. Lunkwitz, *Nucl. Instrum. Methods Phys. Res., Sect. B*, 2000, **161**, 1154–1158.
- 34 D. Pospiech, A. Korwitz, H. Komber, D. Voigt, D. Jehnichen, J. Müller, A. Janke, T. Hoffmann and B. Kretzschmar, *High Perform. Polym.*, 2007, **19**, 565–580.
- 35 T. Köppl, S. Brehme, D. Pospiech, O. Fischer, F. Wolff-Fabris, V. Altstädt, B. Schartel and M. Döring, *J. Appl. Polym. Sci.*, 2013, **128**, 3315–3324.
- 36 D. Pospiech, A. Korwitz, H. Komber, D. Jehnichen, L. Häußler, H. Scheibner, M. Liebmann, K. Jähnichen and B. Voit, *Macromol. Chem. Phys.*, 2015, **216**, 1447–1461.
- 37 N. S. Murthy, S. T. Correale and H. Minor, *Macromolecules*, 1991, **24**, 1185–1189.
- 38 A. A. Gaonkar, V. V. Murudkar and V. D. Deshpande, *Thermochim. Acta*, 2020, **683**, 178472.
- 39 D. Pospiech, D. Jehnichen, H. Komber, A. Korwitz, A. Janke, T. Hoffmann, B. Kretzschmar, L. Häußler, U. Reuter, M. Döring, S. Seibold, R. Perez-Graterol, J. K. W. Sandler, V. Altstädt, F. Bellucci and G. Camino, *J. Nanostruct. Polym. Nanocompos.*, 2008, **4**, 62–75.
- 40 A. Mehta, U. Gaur and B. Wunderlich, *J. Polym. Sci., Part B: Polym. Phys.*, 1978, **16**, 289–296.
- 41 H. Yoon, L. F. Charbonneau and G. W. Calundann, *Adv. Mater.*, 1992, **4**, 206–214.
- 42 H. R. Kricheldorf and G. Schwarz, *Polymer*, 1984, **25**, 520–528.
- 43 H. T. H. Nguyen, M. H. Reis, P. Qi and S. A. Miller, *Green Chem.*, 2015, **17**, 4512–4517.
- 44 B. J. Holland and J. N. Hay, *Polymer*, 2002, **43**, 1835–1847.
- 45 H. Sun, Y. D. Young, S. Kanehashi, K. Tsuchiya, K. Ogino and J. Sim, *J. Fiber Sci. Technol.*, 2016, **72**, 74–79.

